# Deuterium depth profiles in metals using imaging field desorption*

J. A. Panitz

*Sandia Laboratories, Albuquerque, New Mexico 87115*

(Received 21 September 1976; in final form 1 November 1976)

Depth profiles of 80-eV deuterium ions implanted *in situ* into (110) tungsten have been measured by imaging, field-desorption mass spectrometry. The relative abundance of deuterium was measured from the surface to a depth of 300 Å with 2-Å depth resolution by controlled field evaporation of the specimen, and time-of-flight mass spectroscopy. The measured position of the depth-distribution maximum (49 ± 2 Å from the surface), and structure in the distribution is consistent with a model which describes channeling of the deuterium in the near-surface region following recoil implantation of impurity species from the tungsten surface. The depth distribution of these implanted surface species has also been measured. For carbon and oxygen, penetration is limited to 22 Å, with abundance decreasing exponentially from the surface. The maximum measured implantation depths of these species are in agreement with those predicted theoretically, assuming a model where surface carbon and oxygen are channeled into the near-surface region by the incoming deuterium. These results will be interpreted in the context of the CTR first-wall impurity problem, and will be used to suggest a novel method for *in situ* characterization of low-energy plasma species in operating CTR devices.

PACS numbers: 61.80.Jh, 61.70.Wp

## INTRODUCTION

The study of low-energy ions, implanted in the near-surface region of metallic solids, is of intrinsic interest as well as practical importance. With our recent national commitment to develop the fusion reactor as an alternate energy source, understanding low-energy ion and neutral interaction with metals has become increasingly important. It is now recognized that low-energy species, escaping from the magnetically confined plasma of Tokomak devices, may interact with the surface of the containment vessel to release impurities back into the plasma.[1] The effect of these impurities is to lower the plasma temperature and prevent a DT "burn." An additional (but less obvious) consequence of first-wall interactions is a change in the composition of the near-surface region of the first wall, which may promote material failure or encourage chemical reactions at its surface. Although techniques exist for studying implantation effects at medium- and high-implant energies,[2] low-energy (<100 eV) implantation effects (which occur within the first 100 Å of the surface) are difficult to study. The reason is twofold. First, conventional surface analytic techniques which do not employ mass spectrometers (e.g., Auger spectroscopy) cannot directly detect the presence of hydrogen and helium, the species of prime interest. Second, of those techniques which can detect hydrogen and helium and are surface sensitive (e.g., the ion microprobe), no reliable method exists for depth profiling the near-surface region with sufficient depth resolution. It is obvious that if the range of the implanted species is less than 100 Å, depth resolution better than 10 Å will be necessary to provide accurate depth profiles. Since surface morphology and crystallography are expected to affect the depth distribution of low-energy implants (e.g., channeling probability increases at low energies[3]), it would be of additional benefit to characterize the substrate on an atomic scale. Although low-energy-electron diffraction (LEED) can provide details of atomic regularity, it cannot characterize local variations from crystal symmetry which may significantly affect the local concentration of implanted species.

In order to provide surface characterization on an atomic scale and depth profiling of low-energy-implanted species with angstrom resolution, imaging field-desorption mass spectroscopy[4] (IFDEMS) has been used. In this paper the first examination of 80-eV deuterium ions implanted into tungsten is presented with sufficient resolution (2 Å) to provide a detailed depth distribution within the first hundred angstroms of the surface.

To estimate the amount of deuterium residing on the surface after implantation (as opposed to being distributed in depth) several control experiments have also been performed. These were designed to measure differences in the composition of the surface layer due to residual gas adsorption from the ambient vacuum with, and without, implantation.

## EXPERIMENTAL PROCEDURE

The general outline of the experimental procedure followed is given below. Specific details of the procedure will be presented in later discussions.

A field-ion specimen of (110) tungsten is prepared[5] and its surface crystallography determined by conventional field-ion microscopy.[6] The specimen is chosen so that its radius of curvature, prior to implantation, is below 200 Å. After performing an experiment to determine the identity and abun-

  

dance of surface species due to residual gas adsorption at 300 K, the specimen is implanted (*in situ*, at 300 K) with 80-eV deuterium ions. A system pressure of less than $1 \times 10^{-8}$ Torr ($1.3 \times 10^{-6}$ Pa) is maintained during the implantation. Within five minutes of the implantation, the specimen is cooled to 80 K. (Specimen cooling minimizes the possibility of diffusion within the near-surface region during analysis.) After cooling, the abundance of species on the surface is again determined, and compared to the results prior to implantation in order to determine the effect of implantation on surface composition.

To obtain depth profiles, successive field-evaporation[7] events are initiated in vacuum [$8 \times 10^{-10}$ Torr ($1.1 \times 10^{-7}$ Pa)] to remove, in a controlled fashion, layer-by-atomic-layer of the tungsten lattice. In practice, it is convenient to adjust the evaporation rate so that a fraction (0.3–0.5) of a (110) layer is removed during each desorption event. In order to determine the composition of each complete (110) layer removed, the abundances of species (obtained from a mass spectra) in each partial layer are summed. Depth within the lattice is determined by visually noting successive collapses of the (110) plane in the desorption image which accompanies each desorption event. Each collapse of the (110) plane corresponds to a successively deeper, known penetration into the lattice [2 Å, the (110) interlayer spacing]. In effect, precise depth determination is assured by a series of visual markers [the successive collapses of the (110) plane], with depth resolution equal to the (110) interlayer spacing. The experiment continues until the specimen radius has increased to such an extent that mass resolution suffers,[8] or until the depth profiles no longer exhibit structure. It should be noted that although field-desorbed species are detected primarily from the (110) region, contributions from neighboring crystallographic areas are detected as well. The magnitude of these contributions is determined by the specimen radius and the acceptance angle of the detector.[8] During a depth-profile experiment the specimen radius is increased by successive field-evaporation events. As a result, an increasingly larger fraction of the total specimen area is imaged at the detector so that the abundance of a particular species is not strictly a function of depth, but is modified by continually increasing contributions from neighboring crystallographic areas. Although small, these contributions may affect the details of structure observed in the depth profiles.

## THE VACUUM SYSTEM

Figure 1 is a schematic diagram of the field-desorption spectrometer employing a separate implantation and spectrometer chamber, an isolation valve, and a linear-motion manipulator used to transfer the specimen between chambers. The implantation source is provided with a linear motion feedthrough to allow it to be positioned opposite (facing) the specimen during implantation, and to be withdrawn during specimen transfer. A double-trapped oil-diffusion and getter-ion pump evacuate the source chamber to $8 \times 10^{-8}$ Torr ($1.1 \times 10^{-5}$ Pa) in 15 min following specimen insertion. A getter-ion pump in the spectrometer chamber maintains a pressure of less than $8 \times 10^{-10}$ Torr ($1.1 \times 10^{-7}$ Pa) during

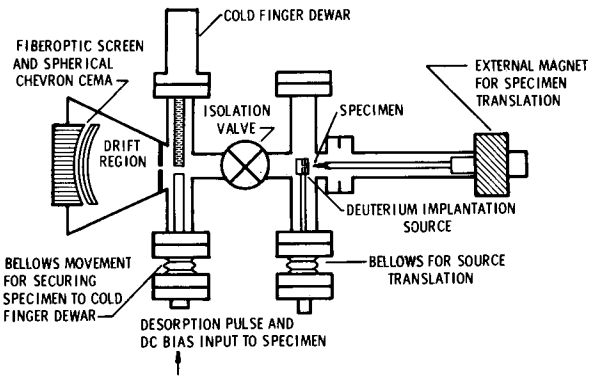


FIG. 1. Schematic diagram of the imaging field-desorption mass spectrometer, employing a spectrometer and implantation chamber separated by an isolation valve. An external magnet provides internal translational motion of the specimen between chambers. The implantation source can be positioned to face the specimen to provide implantation along the specimen axis. Two separate pumping systems are used. The total specimen transfer time from atmosphere in the source chamber to $5 \times 10^{-10}$ Torr ($6.7 \times 10^{-8}$ Pa) in the spectrometer chamber, is less than 30 min.

a profile experiment. When the isolation valve is opened for specimen transfer, the pressure in the spectrometer chamber remains below $5 \times 10^{-9}$ Torr ($6.7 \times 10^{-7}$ Pa). Isolating the spectrometer and source chambers also provides for rapid specimen interchange. The total specimen-transfer time from atmosphere in the source chamber to $5 \times 10^{-10}$ Torr ($6.7 \times 10^{-7}$ Pa) in the spectrometer chamber is less than 30 min.

## THE CONTROL EXPERIMENTS

Two independent experiments were performed in order to determine the abundance of species adsorbed on the specimen surface from the residual gas in each chamber. The adsorption experiment in the source chamber was performed to identify the residual-gas species adsorbed on the specimen surface under implantation conditions, but prior to implantation. The experiment in the spectrometer chamber was designed to determine the magnitude of bulk impurities in the near-surface region of the specimen, and residual-gas adsorption on its surface under the conditions of a depth-profile experiment. During a depth-profile experiment each desorption pulse applied to the specimen removes an appreciable fraction of an atomic layer. In addition to implanted species and bulk impurities, residual-gas species adsorbed on the specimen (after application of the previous desorption pulse) are also removed. Therefore, the spectrometer chamber control experiment determines an upper limit on the species expected to be detected during depth profiling *which do not result from implantation*. Consequently, it provides a reference or "noise" level above which a species abundance must be observed in order to verify that it was implanted into the lattice.

In practice, each control experiment proceeds as follows. The specimen is transferred to the spectrometer chamber and a helium field-ion image is obtained at 80 K [$p_{\text{helium}} = 7 \times 10^{-7}$ Torr ($9.3 \times 10^{-5}$ Pa)] to determine specimen orientation and verify crystal perfection. The helium is then removed [$p = 8 \times 10^{-10}$ Torr ($1.1 \times 10^{-7}$ Pa)] and the specimen is pulsed[9] (and its dc bias increased) until gentle field evaporation of the

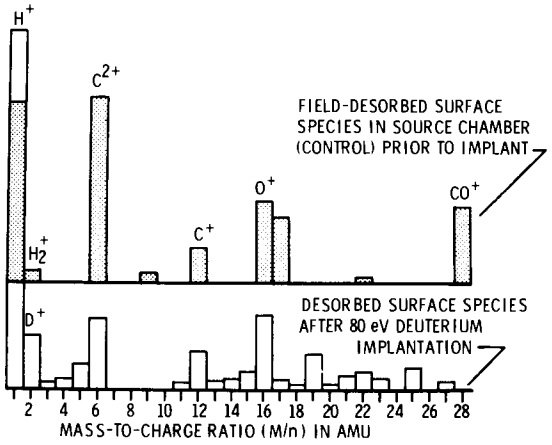


FIG. 2. Upper histogram—Histogram resulting from the source-chamber control experiment showing all species and their abundances caused by adsorbing residual gas on the grounded specimen at 300 K in the implantation chamber [$p = 1 \times 10^{-8}$ Torr ($1.3 \times 10^{-6}$ Pa)]. The adsorption time was chosen to be several times that required to implant the specimen in order to place an upper limit on the abundance of species adsorbed during an implantation. Lower histogram—Histogram of surface species found on the tungsten specimen after implantation with 80-eV deuterium at 300 K (specimen grounded during implantation). The peak at $m/n = 2$ has increased over that obtained in the control experiment, the increase due to deuterium residing on the surface. Both histograms shown in this figure are plotted against the same vertical and horizontal scales. The $H^+$ peak in the lower histogram extends beyond the corresponding peak in the upper histogram.

lattice is observed by the characteristic desorption image of (110) tungsten. The dc specimen potential $V_0$ needed to pulse-field evaporate the lattice at this rate (the rate to be established during the implantation experiment) is recorded.

For the spectrometer-chamber control experiment, the specimen remains in the spectrometer chamber (at specimen potential $V_0$) for the required adsorption time. An evaporation pulse is then applied and the mass spectrum of the desorbed ions recorded. A second pulse (of the same amplitude) is applied immediately after the first, and the resulting spectrum recorded in order to confirm that all species were removed by the previous pulse. This procedure is performed several times to ensure that the species and abundances obtained are characteristic, with the specimen biased at $V_0$.

For the source-chamber control experiment, the specimen is transferred to the source chamber following helium-ion imaging, and establishing a dc desorption potential $V_0$. Since the specimen-transfer mechanism is massive, and at 300 K, the specimen quickly warms to ambient temperature. Following adsorption in the source chamber, the specimen is transferred to the spectrometer chamber, cooled to 80 K, and a desorption pulse applied with a specimen bias of 250 V. The mass spectrum of the desorbed species is recorded, and the specimen bias increased by 250 V. This sequence is repeated (and a mass spectrum recorded) until a specimen potential of $(V_0 - 250)$ V is reached.[10] The relative abundances of the species may change at each different specimen bias corresponding to selective and characteristic desorption fields for each species. But the species and their abundances obtained from each spectrum can be summed and displayed as a composite histogram (upper, "shaded" histogram, Fig. 2) to show all species adsorbed on the surface. This procedure is followed since immediately raising the specimen bias from zero to $(V_0 - 250)$ would remove all weakly bound species prior to pulse desorption. A 250-V increase in specimen bias (much smaller than the desorption-pulse amplitude of 583 V) was chosen to eliminate the possibility of dc desorption of weakly bound species during specimen bias increase. Observation of the phosphor screen of the spectrometer detector while the dc specimen potential was increased by 250 V verified that no surface species were being dc desorbed.

The upper histogram in Fig. 2 is characteristic of the residual-gas species adsorbed on the specimen (at 300 K) in the source chamber. Therefore, it identifies the surface species encountered by the deuterium during the implantation process and provides an upper limit on their relative abundances. Carbon monoxide (CO), carbon, and oxygen are the predominant surface contaminants in addition to hydrogen. The extent to which the impacting deuterium interacts with these species will be discussed shortly. It should be noted that adsorbed species with $m/n > 28$ had very small abundances. In particular, $CO_2$ ($m/n = 44$) had an abundance which was always observed to be at least two orders of magnitude less than that of CO.

The results of the spectrometer-chamber control experiment differed in that surface species characteristic of field evaporating the lattice (following residual-gas adsorption with the specimen biased at $V_0$) were observed. No residual gas species with $m/n > 4$ were observed. A large peak at $m/n = 1$ was recorded, as well as small peaks at $m/n = 2$, 3, and 4. These result from desorption of omnipresent hydrogen (as $H^+$), $H_2^+$ and $H_3^+$ (characteristic field-desorption species having small abundances at most field strengths), and $He^+$ (helium field adsorbed on the surface from residual gas remaining after prior ion imaging of the specimen). The occurrence of $H_2^+$ is important in that it establishes a threshold or "noise" level for the detection of deuterium during depth profiling (implanted deuterium cannot be distinguished in our mass spectra from adsorbed $H_2$).

In the control-chamber histogram (upper histogram of Fig. 2), a small peak due to $H_2^+$ is also seen, and again serves as a threshold level, but for the existence of $m/n = 2$ residing on the surface. An increase in $m/n = 2$ abundance above this level after implantation would correspond to deuterium residing on the surface.

## SURFACE COMPOSITION AFTER IMPLANTATION

Following the control experiments, the specimen is ion imaged in helium and a new $V_0$ established following the removal of the helium [$p = 8 \times 10^{-10}$ Torr ($1.1 \times 10^{-7}$ Pa)]. The specimen is then transferred to the source chamber and the grounded specimen implanted [at 300 K and $1 \times 10^{-8}$ Torr ($1.3 \times 10^{-5}$ Pa)] with 80-eV deuterium ions.[11] It is then transferred to the spectrometer chamber and cooled to 80 K. To determine the residual-gas species residing on the surface, an experiment identical in procedure to that described for the source-chamber control is performed. That is, the specimen potential is increased in 250-V steps to $(V_0 - 250)$ V, with a mass spectrum recorded at each step. For example, Fig. 3 is the eleventh time-of-flight spectrum recorded (specimen bias

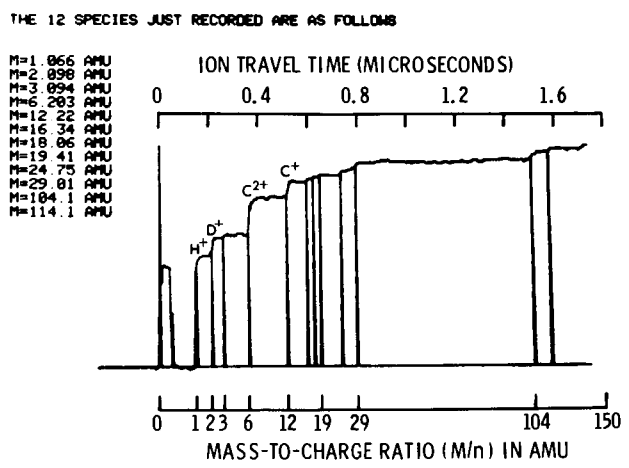


FIG. 3. An arrival-time spectrum of species recorded after implantation of the grounded tungsten specimen with deuterium (at 300 K). This is one of a sequence of detector waveforms obtained prior to field desorption of the first atomic layer of the specimen, used to characterize the species residing on the surface. A computer printout of the detected species is displayed with their positions (indicated by vertical lines intersecting the waveform). The height of a step (corresponding to a species arrival) is proportional to its abundance. Time (and mass) is measured from a fiducial marker superimposed on the waveform during the experiment. $V_{specimen} = 2.75$ kV, $V_{pulse} = 583$ V, $V_0$ (the potential which will cause field evaporation of the specimen) $= 4.93$ kV, $p = 8 \times 10^{-10}$ Torr ($1.1 \times 10^{-7}$ Pa), $T = 80$ K. All time of flight measurements and computer analyses are made with a Tektronix-type WP2321 Waveform Processing System.

$= 2.75$ kV, $V_{pulse} = 583$ V, $V_0 = 4.93$ kV) after implantation. A computer printout of the masses observed and their position (indicated by the vertical lines intersecting the spectrum) is also shown. A time (and corresponding, mass) scale is superimposed on the printout, each starting at a fiducial time marker recorded with the spectrum (prior to the arrival of $H^+$). Species arrival at the detector are indicated by steps in the waveform, with an abundance for each species proportional to its step height. By summing the abundances of species at all specimen potentials a composite histogram is obtained, and identifies all species present on the surface (and their relative abundances) *following implantation*. This histogram is shown in Fig. 2 (lower histogram), where it is plotted on the same scale used for the source chamber control histogram.

A comparison of the two histograms in Fig. 2 shows several interesting and reproducible features. First, the height of the $m/n = 2$ peak after implantation is essentially four times the height of the $m/n = 2$ peak prior to implantation. If one assumes that the $m/n = 2$ peak height in the control experiment (due to $H_2$) is unaffected by the implantation process, then the $H_2$ peak height can be subtracted from the $m/n = 2$ peak height observed after implantation. The result definitely establishes the existence of deuterium residing on the surface after implantation. Furthermore, the surface deuterium peak height can be compared with the maximum deuterium peak height observed during the subsequent depth-profile measurement of deuterium. The comparison establishes that the amount of deuterium on the surface is more than one third of the maximum deuterium detected in any atomic layer of the near-surface region probed during the depth analysis.

A second noticeable feature in the histograms of Fig. 2 is the disappearance of surface CO following implantation. This appears to be characteristic of the implantation process. Since carbon and oxygen peak heights do not increase after implantation, one can safely assume that adsorbed CO is not dissociating at the surface as a result of the 80-eV deuterium bombardment. It is possible that the CO molecule is desorbed from the surface during the 80-eV ion bombardment, but another possibility exists which is consistent with an unanticipated result of the depth-profile measurements: a depth distribution of carbon and oxygen in the near-surface region. These profiles suggest that surface CO is driven into the near-surface region by the implanting deuterium ions.

Another related feature of a comparison of the histograms in Fig. 2 is a decrease of one of the carbon peaks ($C^{2+}$) after implantation. This species, also observed in subsequent depth profiles, provides another example of a surface species driven into the near-surface region by the implanting deuterium.

## THE IMPLANTATION PROFILES

Figure 4 is a depth profile of $C^+$, $C^{2+}$, $O^+$, and deuterium, observed in the near-surface region after implantation. An abundance for $C^+$, $C^{2+}$, and $O^+$ at the surface was obtained by extrapolating the depth-profile curves for these species to the surface. Assuming that the implanted C and O originated by forcing surface CO into the near-surface region, the CO peak height obtained (from the extrapolated surface $C^+$ and $O^+$ abundances) is essentially equal to the height of the CO peak, *which disappeared after implantation*, in the control experiment. If one calculates the penetration depth of surface carbon (or oxygen) under 80-eV deuterium bombardment using an amorphous solid model (no crystallography), a maximum depth of less than 10 Å is obtained.[12] However, if channeling of these species is assumed, and a calculation

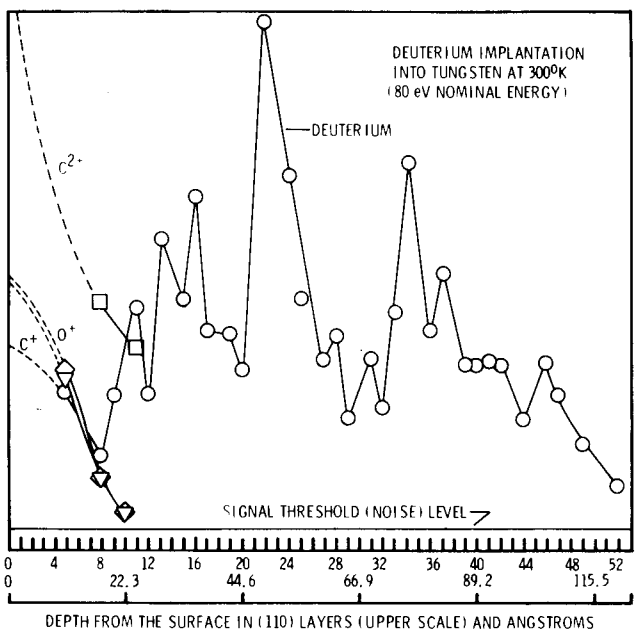


FIG. 4. Depth profiles of $C^{2+}$, $C^+$, $O^+$, and $D^+$ in the near-surface region of (110) tungsten, following implantation with 80-eV deuterium at 300 K. Depth is measured at discrete steps corresponding to the removal of one (110) layer from the specimen. Depth resolution is determined by the (110) interlayer spacing (2.2 Å). The specimen was cooled to 80 K to prevent species migration during the time necessary to obtain the profile.

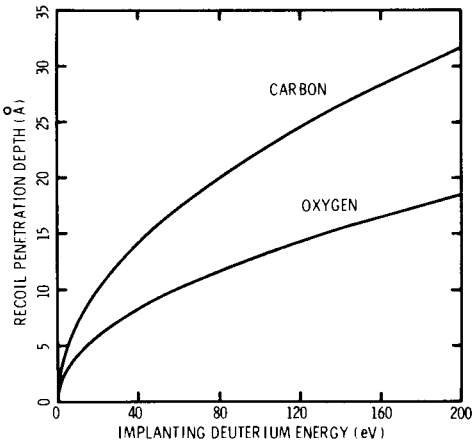


FIG. 5. Theoretical calculation of the maximum range of recoil implanted carbon and oxygen in tungsten assuming channeling of the implanted species in a free-electron gas (D. K. Brice, Sandia Laboratories, Albuquerque, NM).

made[12] using a free-electron gas approximation,[13] the maximum penetration depth of carbon and oxygen in tungsten agrees with the experimental data of Fig. 4. The results of such a calculation[12] are shown in Fig. 5. For 80-eV deuterium, the agreement between the predicted implanted depth of carbon (20 Å), and that measured [ten (110) layer spacing $\cong$22 Å], is excellent. For oxygen, the agreement is fair, with the experiment measuring a depth equal to that of carbon, and theory predicting a depth for oxygen $\approx$40% less than that of carbon. This discrepancy may be due to neglecting the effect of differences in the shell structure of carbon and oxygen when calculating the penetration depths in Fig. 5. At low implant energies, shell-structure effects have been measured for carbon and oxygen in silicon.[14] If true for tungsten, the difference in the predicted penetration depths for carbon and oxygen (at a given deuterium energy) would become smaller than shown in Fig. 5, in better agreement with the experimental measurements.

The $C^{2+}$ depth profile when extrapolated to the surface gives a surface abundance of $C^{2+}$, which is essentially equal to the difference between the $C^{2+}$ peak heights in Fig. 2 before and after implantation.

*We believe that these results are the first direct experimental observation of recoil implantation of surface species into the near-surface region by low-energy ion bombardment.*[15]

A theoretical description of the form of the deuterium profile of Fig. 4 is beyond the scope of this paper, but will be discussed elsewhere.[16] Here, only a summary of the main features of the theoretical analysis will be presented. First, the profile appears to have a primary maximum[17] centered at the 22nd layer (49 $\pm$ 2 Å from the surface). Its position is consistent with the maximum penetration of 80-eV deuterium channeled into tungsten.

The second (and most striking) feature of the profile is an unanticipated, sharply peaked distribution in depth. Such structure is reproduced by the theoretical calculations, and can be attributed to scattering of deuterium by surface species into preferred channels of the tungsten crystal (allowed crystallographic directions).

## CONCLUSIONS

It has been shown that it is possible to accurately measure the composition of the first monolayer of a tungsten specimen before and after 80-eV deuterium implantation. Together with depth profiles of carbon and oxygen in the near-surface region, the disappearance of surface CO (and the decrease of $C^{2+}$) after implantation can be attributed to recoil implantation in the near-surface region. A theoretical prediction of the maximum penetration depth of carbon and oxygen is in good agreement with experiment, providing channeling of the carbon and oxygen is assumed. The implanted deuterium profile can be explained if one assumes that the deuterium is channeled into the near-surface region following scattering by adsorbed surface species. Peaks in the deuterium profile are explained in such a model by selective scattering into preferred crystal channels.

Since the position of the maximum (and the width) of an implantation profile reflects the energetic characteristics of the implanting source (and will not discriminate against energetic neutrals), it may be possible to use such profiles to characterize the low-energy species which escape from the magnetically confined plasma of Tokomak devices and strike the first wall. Using several *in situ* specimens (located at the first wall and biased to different potentials) low-energy neutral species can be separated from their charged companions and given a reasonably accurate theoretical prediction of maximum implant depth versus energy, an energy spectrum of the implanting species can be obtained. Of course, such an analysis is predicted upon the specimens' ability to survive a hostile[8] CTR environment, while preserving identifiable crystallographic features which are necessary for an accurate determination of a depth scale.

## ACKNOWLEDGMENTS

The author wishes to acknowledge the perseverence and stamina of R. J. Walko, who assisted in performing these experiments, as well as the technical expertise of G. E. Fowler who constructed much of the implantation spectrometer. D. K. Brice was instrumental in interpreting the structure of the measured depth distributions, and the author would like to acknowledge many fruitful discussions with him.

*This work was supported by the Controlled Thermonuclear Reaction Division of ERDA.

[1]R. Behrisch and B. B. Kadomtsev, *Plasma Physics and Controlled Nuclear Fusion Research 2* (International Atomic Energy Agency, Vienna, 1975), p. 229.

[2]M-A. Nicolet, J. W. Mayer, and I. V. Mitchell, Science **177**, 841 (1972).

[3]D. S. Gemmel, Rev. Mod. Phys. **46/1**, 129 (1974).

[4]J. A. Panitz, J. Vac. Sci. Technol. **11**, 206 (1974).

[5]Electrochemical etching of 0.1-mm-diam tungsten wire in 10% NaOH + 90% $NH_4OH$ (3–15 V ac).

[6]E. W. Muller and T. T. Tsong, *Field Ion Microscopy, Principles and Applications* (Elsevier, New York, 1969).

[7]Field evaporation refers specifically to the removal of *lattice* atoms in a high electric field. Field desorption refers to the more general field-induced removal of any substrate species.

[8]J. A. Panitz, J. Nucl. Mater. (in press).

[9]The desorption-pulse amplitude (at the specimen) used for the control experiments was identical to that used during implantation (583 V).

[10]Pulsing 250 V below $V_0$ minimized the possibility of lattice evaporation,

while assuring that all adsorbed surface species would be removed.

[11]The total number of implanting deuterium ions was estimated to be less than 300, insuring that no appreciable lattice damage would occur as a result of the implantation.

[12]D. K. Brice, Sandia Laboratories, Albuquerque, NM (private communication).

[13]J. Lindhard, Kgl. Danske Videnskab. Selskab, Mat. Fys. Medd. **28/8** (1954).

[14]F. H. Eisen, Can. J. Phys. **46/6**, p. 561.

[15]Although this conclusion is consistent with the data, an alternate explanation of the experimental results is possible. Since mass separation of the ion-source beam was not attempted, any contaminant of carbon and oxygen in the deuterium ion source which had significantly lower energy than the deuterium could implant along with the deuterium, giving rise to the observed profiles. Of course, a separate mechanism [e.g., selective sputtering of CO and carbon (as $C^{2+}$) by 80-eV $D^+$ ions] would also have to be invoked to explain the complementary decrease of these surface species after implantation.

[16]D. K. Brice, Sandia Laboratories, Albuquerque, NM (to be published).

[17]The deuterium ion beam used in this study may have contained a neutral component which could have implanted along with the deuterium ions. Evidence for a possible second component in the primary beam is a possible secondary maximum at 34 (110) layer spacings (76 Å from the surface) in Fig. 4.